Original Article | Cardiovascular Imaging

https://doi.org/10.3348/kjr.2018.19.4.692
pISSN 1229-6929 · eISSN 2005-8330
Korean J Radiol 2018;19(4):692-703

Korean Journal of Radiology
KJR

Is It Better to Enter a Volume CT Dose Index Value before or after Scan Range Adjustment for Radiation Dose Optimization of Pediatric Cardiothoracic CT with Tube Current Modulation?

Hyun Woo Goo, MD, PhD

Department of Radiology and Research Institute of Radiology, University of Ulsan College of Medicine, Asan Medical Center, Seoul 05505, Korea

Objective: To determine whether the body size-adapted volume computed tomography (CT) dose index (CTD_{vol}) in pediatric cardiothoracic CT with tube current modulation is better to be entered before or after scan range adjustment for radiation dose optimization.

Materials and Methods: In 83 patients, cardiothoracic CT with tube current modulation was performed with the body size-adapted $CTDI_{vol}$ entered after (group 1, n = 42) or before (group 2, n = 41) scan range adjustment. Patient-related, radiation dose, and image quality parameters were compared and correlated between the two groups.

Results: The $CTDI_{vol}$ after the CT scan in group 1 was significantly higher than that in group 2 (1.7 ± 0.1 mGy vs. 1.4 ± 0.3 mGy; $p < 0.0001$). Image noise (4.6 ± 0.5 Hounsfield units [HU] vs. 4.5 ± 0.7 HU) and image quality (1.5 ± 0.6 vs. 1.5 ± 0.6) showed no significant differences between the two ($p > 0.05$). In both groups, all patient-related parameters, except body density, showed positive correlations ($r = 0.49–0.94$; $p < 0.01$) with the $CTDI_{vol}$ before and after the CT scan. The $CTDI_{vol}$ after CT scan showed modest positive correlation ($r = 0.49$; $p \leq 0.001$) with image noise in group 1 but no significant correlation ($p > 0.05$) in group 2.

Conclusion: In pediatric cardiothoracic CT with tube current modulation, the $CTDI_{vol}$ entered before scan range adjustment provides a significant dose reduction (18%) with comparable image quality compared with that entered after scan range adjustment.

Keywords: *Radiation dose optimization; Cardiac CT; Tube current modulation; Child; Image quality evaluation*

INTRODUCTION

Various radiation dose reduction techniques have been developed and used to minimize computed tomography (CT) radiation dose while maintaining diagnostic image quality which is especially crucial in pediatric CT (1-3). Among them, attenuation-based tube current modulation technique is useful to reduce radiation dose without substantial increase in image noise (4-7). To use the technique properly in clinical practice, we should first recognize the unique relationships between image noise and image quality indicators between different tube current modulation techniques (8). In all systems, a user-determined image quality level is required for CT scanning with tube current modulation. In body size-adapted CT protocols particularly important in children having a great diversity in body size and habitus, the user-determined image quality level should be adjusted by using one of various body size indices, including body weight, body mass index, cross-sectional dimensions, and body attenuation. In this regard, cross-sectional dimensions, such as area and circumference, are

Received November 10, 2017; accepted after revision January 5, 2018.

Corresponding author: Hyun Woo Goo, MD, PhD, Department of Radiology and Research Institute of Radiology, University of Ulsan College of Medicine, Asan Medical Center, 88 Olympic-ro 43-gil, Songpa-gu, Seoul 05505, Korea.
• Tel: (822) 3010-4388 • Fax: (822) 476-0090
• E-mail: ghw68@hanmail.net

Korean Journal of Radiology
KJR

superior to body weight in body size-adapted CT radiation dose optimization (9, 10). On the other hand, patient attenuation as estimated from CT scout image may be used to determine body size, but proper calibration process, no use of edge-enhancing filters, and exact patient centering are required to avoid errors in the size estimation (11-13). Consequently, the axial CT image-based method is easier and straightforward in estimating patient attenuation than the CT scout image-based method (12, 13).

In a prior study (14), volume CT dose index ($CTDI_{vol}$) as the user-determined image quality indicator was individually determined by the cross-sectional area (A_{body}) and mean body density (D_{body}), and more uniform image noise of contrast-enhanced pediatric chest CT could be achieved when scanned with a combined tube current modulation. In the study, the user-determined $CTDI_{vol}$ value was entered after the scan range adjustment (14). However, it may be more appropriate from the point of view of CT radiation dose optimization if the $CTDI_{vol}$ value was first entered at the same axial position where the A_{body} and mean D_{body} were calculated and the scan range was extended later from the minimum to the full. Therefore, this study was aimed to determine whether the $CTDI_{vol}$ value based on A_{body} and mean D_{body} in pediatric cardiothoracic CT with tube current modulation was better to be entered before or after scan range adjustment for CT radiation dose optimization.

MATERIALS AND METHODS

Study Population

This retrospective study was approved by the local Institutional Review Board and informed consent was waived. Between April 2010 and September 2010, 83 consecutive patients who underwent dual-source cardiothoracic CT examinations (SOMATOM Definition; Siemens Healthineers, Forchheim, Germany) were included in this study. In cardiothoracic CT, $CTDI_{vol}$ based on a 32-cm phantom was individually determined by a best fit equation based on A_{body} and mean D_{body} measured from an axial CT image obtained with the same imaging parameters (80 kV, 25 mA, $CTDI_{vol}$ 0.3 mGy, gantry rotation time 0.33 s, slice thickness 10 mm, and B30f kernel) and approximately 1–2 cm above the dome of the liver for bolus tracking (Fig. 1), as described in a previous study (14). In all patients, the same cardiothoracic scan range from the thoracic inlet to the first lumbar vertebra, 80 kVp, 34 x 0.6 mm detector collimation with z-flying focal spot, pitch 1, and an iterative reconstruction in image space (IRIS; Siemens

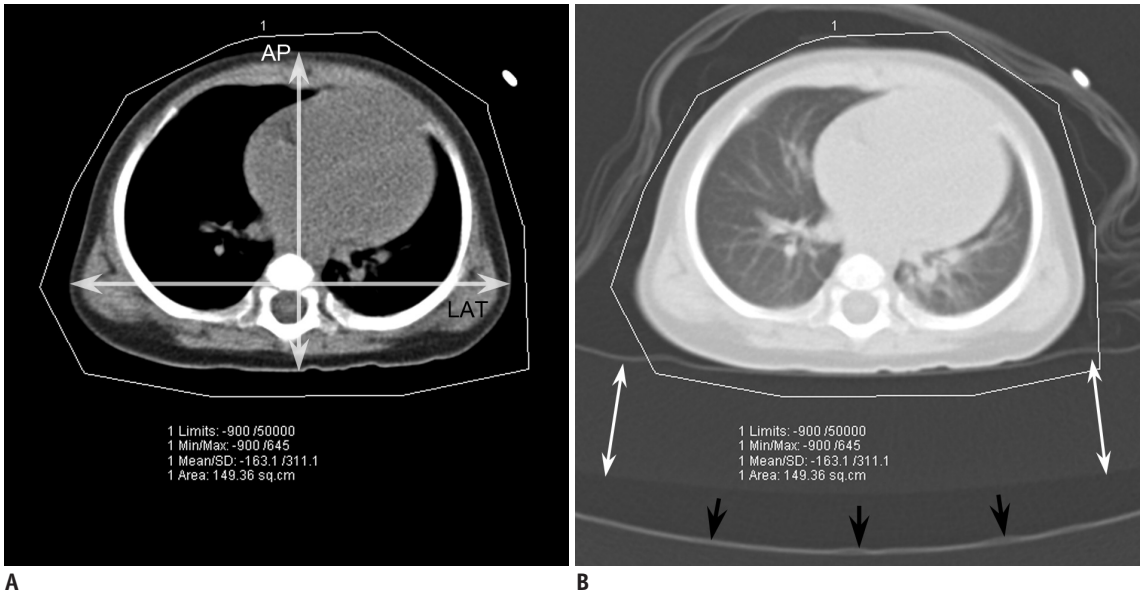

A B

Fig. 1. Axial CT image obtained approximately 1–2 cm above dome of liver in which X-ray output in $CTDI_{vol}$ based on 32-cm phantom was individually determined. To measure area and mean density, CT technologist draws region of interest to include entire patient cross-section with upper (50000 HU) and lower (-900 HU) limits of CT numbers.
A. On same axial CT image with mediastinal window setting, AP was measured from most anterior body surface to most posterior body surface (vertical arrow) and LAT was measured from most right lateral body surface to most left lateral body surface (horizontal arrow). **B.** On same axial CT image with lung window setting, additional radiolucent pad (white arrow) is shown to be placed on CT table (black arrows) to adjust patient's vertical position at isocenter. Blanket wrapping around patient and patient cloth are shown in lung window. AP = anteroposterior diameter, CT = computed tomography, $CTDI_{vol}$ = volume CT dose index, HU = Hounsfield units, LAT = lateral diameter

Healthineers) strength 5 with a medium smooth kernel (I26f), were used. In addition, combined tube current modulation (CARE Dose 4D; Siemens Healthineers) was turned on in all patients to reduce radiation dose without substantial image degradation. One patient showing severe motion artifacts, one whose head was included in the scan range, and one in which descending aortic enhancement was below 250 Hounsfield unit (HU) were excluded from this study.

In the initial 42 patients (group 1), the individually calculated X-ray output was entered after scan range adjustment (Fig. 2A). In the subsequent 41 patients (group 2), the individually calculated X-ray output was entered with a minimal longitudinal range in the same position as the axial CT image obtained for the X-ray output determination and a full scan range was then adjusted (Fig. 2B, C). In the group 2, the entered $CTDI_{vol}$ value, therefore, was automatically changed to a new value after the scan range adjustment, based on body attenuation information obtained from the CT scout image. As a result, the actual X-ray output used for CT scanning would differ between the two methods in spite of the same user-determined radiation dose input. From the measured A_{body} and mean D_{body} of each patient, water equivalent area (A_w) was calculated by using the following formula:

$$A_w = (D_{body} / 1000 + 1) \times A_{body} \quad (1)$$

On the same axial CT image used for the measurement of A_{body} and mean D_{body}, the anteroposterior diameter (AP) was measured from the most anterior body surface to the most posterior body surface and the lateral diameter (LAT) was measured from the most right lateral body surface to the most left lateral body surface (Fig. 1A). In the measurement of the lateral diameter, an arm was included if it contacted to the body trunk. The effective diameter (D_{eff}) was then calculated by using the following formula:

$$D_{eff} = \sqrt{AP \times LAT} \quad (2)$$

The detailed characteristics of the patients in the two groups are described in Table 1. Patient age and body parameters including A_{body}, D_{body}, A_w, and AP, LAT, and D_{eff} were compared between the two groups, and showed no significant differences between the two (Table 1).

Arm position on the CT scout image was categorized into 'up,' 'horizontal,' and 'down' (Figs. 1, 3). The horizontal position was defined when an angle between the arm and the horizontal axis was less than ± 30°. Proportions of the arm positions appeared comparable between the two groups (Table 1).

Cardiothoracic CT

Prospectively electrocardiography (ECG)-triggered sequential scan was performed during free-breathing in all patients. Additional respiratory triggering, the so-called combined ECG and respiratory triggering, was used with a pressure-sensing belt of a respiratory gating system (AZ-733V; Anzai Medical Co., Ltd., Tokyo, Japan) in 76.2% (32/42) in the group 1 and 61.0% (25/41) in the group

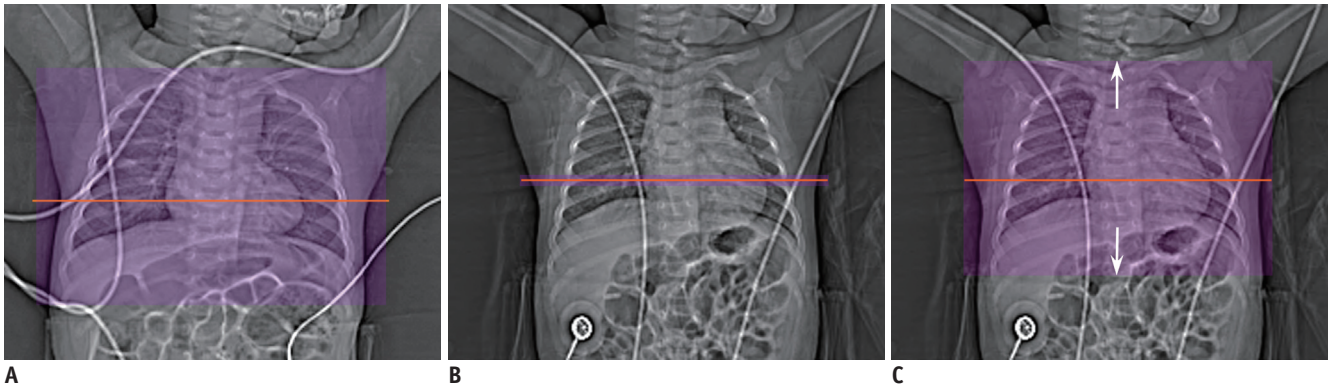

Fig. 2. Comparison of user-determined radiation dose in pediatric cardiothoracic CT with tube current modulation in two groups.
A. CT scout image shows slice position (horizontal orange line) of axial CT image for determination of $CTDI_{vol}$ that was entered after scan range adjustment (transparent purple rectangle) in group 1. **B.** CT scout image shows slice position (horizontal orange line) of axial CT image for determination of $CTDI_{vol}$ that was entered with minimal longitudinal range at same position (transparent purple rectangle) in group 2. **C.** In group 2, scan range was subsequently extended longitudinally (arrows) to full scan range (transparent purple rectangle) of cardiothoracic CT scanning. As result, initially entered $CTDI_{vol}$ value with minimal longitudinal range was automatically changed to new value after scan range adjustment, based on body attenuation information obtained from CT scout image in group 2. Of note, both arms are raised up on CT scout image in both cases.

Korean Journal of Radiology
KJR

Table 1. Patient Characteristics

	Group 1 (n = 42)	Group 2 (n = 41)	*P*
Age	8.0 ± 9.1 months; median, 4 months; range, 1 day–3 years	9.6 ± 14.2 months; median, 4 months; range, 1 day–4 years	0.5
Male to female ratio	25:17	14:27	-
Diagnosis	Tetralogy of Fallot, 18; functional single ventricle, 5; double outlet right ventricle, 5; ventricular septal defect, 3; coarctation of aorta, 3; left pulmonary artery sling, 2; transposition of great arteries, 2; interrupted aortic arch, 1; pulmonary atresia with ventricular septal defect and multiple aortopulmonary collateral arteries, 1; Williams syndrome, 1; negative (suspected vascular ring at echocardiography), 1	Tetralogy of Fallot, 11; coarctation of aorta, 8; functional single ventricle, 5; atrial septal defect, 2; total anomalous pulmonary venous return, 2; double outlet right ventricle, 1; atrial and ventricular septal defects, 1; atrioventricular septal defect, 1; patent ductus arteriosus, 1; interrupted aortic arch, 1; partial anomalous pulmonary venous return, 1; vascular ring, 1; Ebstein anomaly, 1; Williams syndrome, 1; Loeys Dietz syndrome, 1; Allagile syndrome, 1; aortic stenosis, 1; negative (suspected double outlet right ventricle at echocardiography), 1	-
Arm position	Both up, 28; both horizontal, 7; both down, 5; one horizontal and one up, 1; one down and one horizontal, 1	Both up, 25; both horizontal 9; both down, 4; one horizontal and one up, 3	-
A_{body} (cm^2)	149.8 ± 26.4	145.6 ± 53.1	0.6
D_{body} (HU)	-197.0 ± 46.0	-200.6 ± 55.6	0.7
A_w (cm^2)	120.0 ± 20.3	115.6 ± 41.5	0.6
AP (cm)	10.3 ± 1.4	10.1 ± 1.9	0.5
LAT (cm)	15.2 ± 1.5	14.4 ± 2.8	0.1
D_{eff} (cm)	12.5 ± 1.3	12.0 ± 2.0	0.2

A_{body} = cross-sectional area, AP = anteroposterior diameter, A_w = water equivalent area, D_{body} = body density, D_{eff} = effective diameter, HU = Hounsfield unit, LAT = lateral diameter

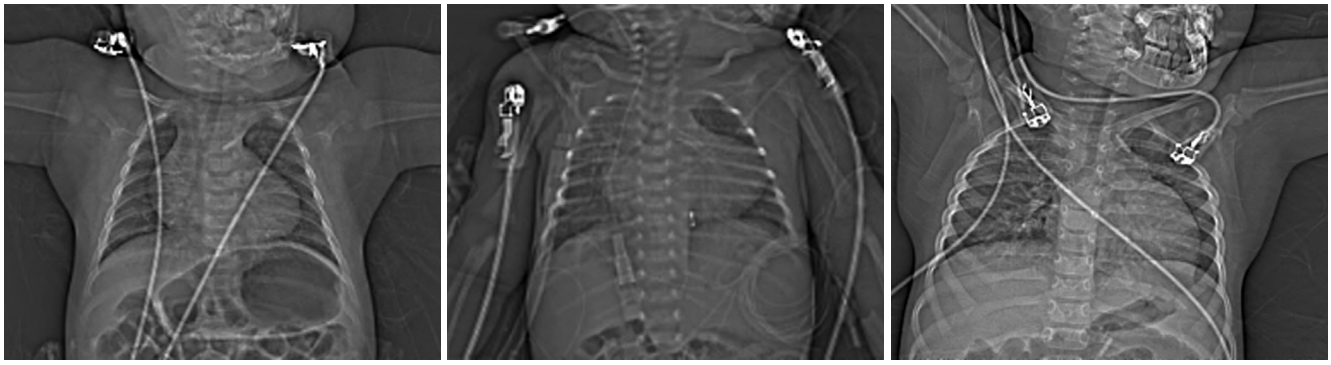

A **B** **C**

Fig. 3. Variable arm positions on CT scout images.
A. CT scout image shows that both arms are horizontal, which is greatly disadvantageous in terms of image quality and radiation dose, as compared with both arms raised up. **B.** CT scout image shows that both arms are down beside body trunk, which may slightly degrade image quality and increase radiation dose, as compared with both arms raised up. **C.** CT scout image shows that right arm is raised up and left arm is horizontal, which may cause asymmetric image quality degradation in left shoulder region and increased radiation dose, as compared with both arms raised up.

2, to reduce respiratory misregistration artifacts between adjacent imaging slabs as previously described (15). ECG electrodes were placed outside the thoracic region as much as possible (Fig. 2) to reduce metal artifacts and potential adverse effect on tube current modulation. Because isocentering of a patient in a CT gantry is crucial for the optimal use of tube current modulation, a radiology technologist adjusted patient position at the isocenter and an additional radiolucent pad was placed upon the CT table for a small child to compensate for low vertical positions even at the maximum CT table height (Fig. 1B) (16). To sedate the patients, oral choral hydrate (50 mg/

kg) was initially used and intravenous midazolam (0.1 mg/kg) or ketamine (1 mg/kg) was additionally administered as needed. Iodinated contrast agent (Iomeron 400, iomeprol 400 mg I/mL; Bracco Imaging SpA, Milan, Italy; 1.5–2.0 mL/kg) was intravenously administered at an injection rate of 0.3–1.0 mL/s by using a dual-head power injector and a tri-phasic injection protocol, in which undiluted contrast agent was followed by 50% diluted contrast agent and then by 5% diluted contrast agent, to achieve uniform cardiovascular enhancement and minimal peri-venous streak artifacts from undiluted contrast agent. The scan delay time was determined by a bolus tracking technique with a trigger threshold of 150 HU in the left ventricular cavity.

Radiation Dose and Image Quality Parameters

The two $CTDI_{vol}$ values, the one determined by the A_{body} and D_{body} and entered before the CT scan, and the other displayed after the CT scan were recorded. Target noise calculated by the best fit equation (14) was recorded. In addition, the displayed effective mAs and quality reference mAs after the CT scan were recorded. At two levels, i.e., 1) the aortic arch and 2) the descending aorta with the same slice position as the axial CT image obtained approximately 1–2 cm above the dome of the liver, CT density was measured in the aorta, spinal muscles, and air by placing rectangular regions of interest in the areas showing homogeneous attenuation as much as possible (Fig. 4A). In particular, a lung window setting was used to avoid patient cloth and blanket in measurements of air density. Although the same tube voltage (80 kVp) was used in all cardiothoracic CT scans, standard deviations of aortic and muscular densities might be affected by a different level of contrast enhancement. Consequently, image noise of the CT images was defined as the standard deviation of the air density. Because variable slice thickness (S) ranging from 0.8 mm to 4 mm was used, the image noise (σ) was normalized to the slice thickness of 3 mm by using the following formula:

$$\sigma 2 \propto 1 / S \quad (3)$$

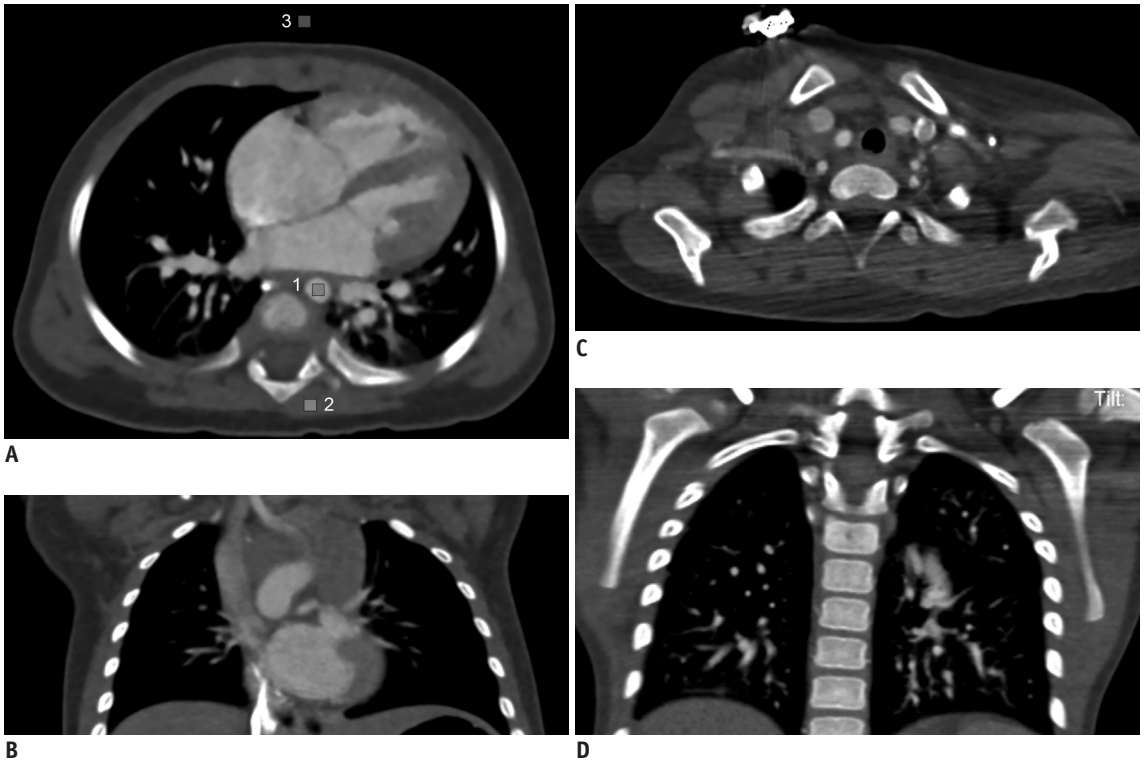

Fig. 4. Subjective image quality grading of pediatric cardiothoracic CT.
Axial **(A)** and coronal **(B)** CT images show excellent image quality (grade 1) without substantial artifacts in 6 months-old female infant whose arm were raised up during CT scanning. Axial CT image **(A)** at same slice position, where $CTDI_{vol}$ value was calculated, was used to measure CT densities in aorta (1), spinal muscles (2), and air (3) by placing rectangular regions of interest in areas showing homogeneous attenuation as much as possible. Axial **(C)** and coronal **(D)** CT images show severely degrade subjective image quality (grade 3) in posterior thoracic inlet and left shoulder regions due to horizontal position of left arm during CT scanning. Metal artifacts from electrocardiography electrode located at right upper chest are also noted on axial CT image **(C)**.

Korean Journal of Radiology
KJR

From mean aortic density (D_{aorta}) and slice thickness-normalized image noise from air density (σ_{air}) of the two measurements, signal-to-noise ratio (SNR) was calculated by using the following formula:

$$SNR = D_{aorta} / \sigma_{air} \quad (4)$$

From mean aortic density (D_{aorta}), muscle density (D_{muscle}), slice thickness-normalized image noise from air density (σ_{air}) of the two measurements, contrast-to-noise ratio (CNR) was calculated by using the following formula:

$$CNR = (D_{aorta} - D_{muscle}) / \sigma_{air} \quad (5)$$

Subjective image quality on axial and coronal CT images was graded on a 3-point scale (grade 1, excellent; grade 2, mildly degraded; grade 3, severely degraded) (Fig. 4) by a pediatric radiologist with 17 years of experience in pediatric cardiothoracic CT.

Statistical Analysis

Continuous variables are presented as mean ± standard deviation or median with range, and categorical variables are expressed as frequency with percentage. Continuous variables were compared between the two groups by using unpaired *t* test. Subjective image quality grades were compared between the two groups by using Mann-Whitney U test. Pearson correlations were performed between patient-related, radiation dose, and image quality parameters in both groups. $CTDI_{vol}$ values before and after the CT scan was compared by using paired *t* test in each group. A *p* value of less than 0.05 was considered to be statistically significant. Statistical analyses were performed by using statistical software (SPSS version 24.0; IBM Corp., Armonk, NY, USA).

RESULTS

Radiation Dose and Image Quality Parameters of Cardiothoracic CT

Radiation dose and image quality parameters of cardiothoracic CT in the group 1 and the group 2 are described in Table 2. $CTDI_{vol}$ values after the CT scan (1.7 ± 0.1 mGy), effective mAs (168.0 ± 10.7), and quality reference mAs (411.0 ± 57.5) in the group 1 were significantly higher than those in the group 2 (1.4 ± 0.3 mGy, 141.0 ± 28.6, and 354.0 ± 50.2; $p < 0.0001$), while $CTDI_{vol}$ values before the CT scan showed no significant difference between the two groups (1.1 ± 0.07 mGy vs. 1.1 ± 0.2 mGy; $p = 1.0$) (Table 2). $CTDI_{vol}$ values after the CT scan were significantly higher than those before the CT scan in both group 1 (1.7 ± 0.1 mGy vs. 1.1 ± 0.07 mGy; $p < 0.0001$) and group 2 (1.4 ± 0.3 mGy vs. 1.1 ± 0.2 mGy; $p < 0.0001$).

Target noise (12.3 ± 0.3 HU vs. 12.2 ± 0.6 HU), slice thickness-normalized image noise (4.6 ± 0.5 HU vs. 4.5 ± 0.7 HU), aortic densities (369.1 ± 90.9 HU vs. 368.5 ± 87.2 HU at the aortic arch, 380.2 ± 77.9 HU vs. 369.6 ± 90.3 HU at the descending aorta), SNR (83.3 ± 19.3 vs. 82.9 ±

Table 2. Radiation Dose and Image Quality Parameters

	Group 1 (n = 42)	Group 2 (n = 41)	*P*
$CTDI_{vol}$ before CT scan (mGy)	1.1 ± 0.1	1.1 ± 0.2	1.0
$CTDI_{vol}$ after CT scan (mGy)	1.7 ± 0.1	1.4 ± 0.3	< 0.0001
Effective mAs	168.0 ± 10.7	141.0 ± 28.6	< 0.0001
Quality reference mAs	411.0 ± 57.5	354.0 ± 50.2	< 0.0001
Target noise (HU)	12.3 ± 0.3	12.2 ± 0.6	0.3
Slice thickness	1.5 mm, 2; 2 mm, 31; 3 mm, 8; 4 mm, 1	0.8 mm, 2; 2 mm, 24; 3 mm, 14; 4 mm, 1	-
Slice thickness-normalized image noise (HU)	4.6 ± 0.5	4.5 ± 0.7	0.7
Density (HU) in the aortic arch	369.1 ± 90.9	368.5 ± 87.2	1.0
Density (HU) in the descending aorta	380.2 ± 77.9	369.6 ± 90.3	0.6
D_{muscle} (HU) at the aortic arch	64.8 ± 11.7	69.6 ± 7.8	0.03
D_{muscle} (HU) at the descending aorta	67.0 ± 9.8	72.3 ± 7.7	0.007
SNR	83.3 ± 19.3	82.9 ± 19.7	0.9
CNR	68.7 ± 18.2	66.9 ± 18.9	0.7
Subjective image quality grade	1.5 ± 0.6	1.5 ± 0.6	0.9

CNR = contrast-to-noise ratio, CT = computed tomography, $CTDI_{vol}$ = volume CT dose index, D_{muscle} = muscle density, SNR = signal-to-noise ratio

19.7), and CNR (68.7 ± 18.2 vs. 66.9 ± 18.9) showed no significant differences between the two groups ($p > 0.05$) (Table 2). In contrast, the muscles in the group 1 showed significantly lower CT densities than those in the group 2 at both the aortic arch and the descending aorta levels (64.8 ± 11.7 HU vs. 69.6 ± 7.8 HU at the aortic arch, 67.0 ± 9.8 HU vs. 72.3 ± 7.7 HU at the descending aorta; $p < 0.05$) (Table 2). Subjective image quality grading in the group 1 was as follows: grade 1, 25; grade 2, 14, grade 3, 3. Subjective image quality grading in the group 2 was similar to that in the group 1 as follows: grade 1, 24; grade 2, 15, grade 3, 2. The subjective image quality grades showed no significant difference between the two groups (1.5 ± 0.6 vs. 1.5 ± 0.6; $p > 0.05$) (Table 2).

Correlations between Patient-Related and Radiation Dose Parameters

Correlations between patient-related and radiation dose parameters in group 1 and group 2 are summarized in Table 3. In both groups, all patient-related parameters, except D_{body}, showed highly positive correlations with $CTDI_{vol}$ values before and after the CT scan as well as effective mAs ($p < 0.01$): the highest ($r = 0.86–0.94$) for A_w and the lowest ($r = 0.49–0.59$) for lateral diameter (Table 3). D_{body} showed significantly higher correlations ($r = 0.46–0.47$; $p = 0.002$) with $CTDI_{vol}$ values before and after the CT scan as well as effective mAs in the group 1, while no significant correlations ($p > 0.05$) were found in the group 2 (Table 3). In the group 1, A_w, A_{body}, anterioposterior and D_{eff}, and age showed modest correlations ($r = 0.40–0.69$; $p < 0.01$) with quality reference mAs, but D_{body} and lateral diameter were noted to have no significant correlations ($p > 0.05$) with quality reference mAs (Table 3). On the contrary, all patient-related parameters showed no significant correlations ($p > 0.05$) with quality reference mAs in the group 2 (Table 3).

Correlations between Patient-Related and Image Quality Parameters

Correlations between patient-related and image quality parameters in group 1 and group 2 are summarized in Table 4. In both groups, all patient-related parameters, except lateral diameter and D_{body}, showed modest positive correlations ($r = 0.32–0.49$; $p < 0.05$) with slice thickness-normalized image noise (Table 4). Lateral diameter showed a marginally positive correlation ($r = 0.31$; $p = 0.049$) with slice-thickness normalized image noise in group 2 but showed no significant correlation ($p > 0.05$) in group 1 (Table 4). In both groups, no significant correlations ($p > 0.05$) were found between D_{body} and slice-thickness normalized image noise (Table 4). In both groups,

Table 3. Pearson Correlation Coefficients (*R*) between Patient-Related Parameters and Radiation Dose Parameters

	$CTDI_{vol}$ before CT Scan	$CTDI_{vol}$ after CT Scan	Effective mAs	Quality Reference mAs
A_w				
Group 1	0.88 ($p < 0.0001$)	0.87 ($p < 0.0001$)	0.88 ($p < 0.0001$)	0.56 ($p = 0.0001$)
Group 2	0.94 ($p < 0.0001$)	0.86 ($p < 0.0001$)	0.86 ($p < 0.0001$)	0.06 ($p = 0.7$)
A_{body}				
Group 1	0.80 ($p < 0.0001$)	0.79 ($p < 0.0001$)	0.80 ($p < 0.0001$)	0.53 ($p = 0.0003$)
Group 2	0.87 ($p < 0.0001$)	0.83 ($p < 0.0001$)	0.83 ($p < 0.0001$)	0.06 ($p = 0.7$)
D_{body}				
Group 1	0.47 ($p = 0.002$)	0.46 ($p = 0.002$)	0.46 ($p = 0.002$)	0.03 ($p = 0.8$)
Group 2	0.22 ($p = 0.2$)	0.02 ($p = 0.9$)	0.02 ($p = 0.9$)	0.04 ($p = 0.8$)
AP				
Group 1	0.82 ($p < 0.0001$)	0.81 ($p < 0.0001$)	0.81 ($p < 0.0001$)	0.69 ($p < 0.0001$)
Group 2	0.89 ($p < 0.0001$)	0.82 ($p < 0.0001$)	0.82 ($p < 0.0001$)	0.04 ($p = 0.8$)
D_{eff}				
Group 1	0.80 ($p < 0.0001$)	0.79 ($p < 0.0001$)	0.80 ($p < 0.0001$)	0.53 ($p = 0.0003$)
Group 2	0.80 ($p < 0.0001$)	0.80 ($p < 0.0001$)	0.80 ($p < 0.0001$)	0.23 ($p = 0.2$)
LAT				
Group 1	0.49 ($p = 0.0009$)	0.50 ($p = 0.0008$)	0.50 ($p = 0.0007$)	0.11 ($p = 0.5$)
Group 2	0.54 ($p = 0.0002$)	0.59 ($p < 0.0001$)	0.59 ($p < 0.0001$)	0.31 ($p = 0.052$)
Age				
Group 1	0.71 ($p < 0.0001$)	0.69 ($p < 0.0001$)	0.70 ($p < 0.0001$)	0.40 ($p = 0.009$)
Group 2	0.77 ($p < 0.0001$)	0.74 ($p < 0.0001$)	0.74 ($p < 0.0001$)	0.04 ($p = 0.8$)

Korean Journal of Radiology
KJR

all patient-related parameters showed no significant correlations ($p > 0.05$) with SNR, CNR, and subjective image quality grade (Table 4).

Correlations between Radiation Dose and Image Quality Parameters

Correlations between radiation dose and image quality parameters in the group 1 and the group 2 are summarized in Table 5. $CTDI_{vol}$ value before the CT scan showed modest positive correlations ($r = 0.37$ and 0.52, respectively; $p < 0.05$) with slice thickness-normalized image noise in the group 1 and group 2 (Table 5). $CTDI_{vol}$ value after the CT scan and effective mAs showed modest positive correlations ($r = 0.49$; $p \leq 0.001$) with slice thickness-normalized image noise in the group 1, while no significant correlations ($p > 0.05$) were found between them in the group 2 (Table 5, Fig. 5). In both groups, quality reference mAs showed no significant correlation ($p > 0.05$) with slice thickness-

Table 4. Pearson Correlation Coefficients (*R*) between Patient-Related Parameters and Image Quality Parameters

	Slice Thickness-Normalized Image Noise	SNR	CNR	Subjective Image Quality Grade
A_w				
Group 1	0.43 ($p = 0.005$)	0.20 ($p = 0.2$)	0.14 ($p = 0.4$)	0.27 ($p = 0.09$)
Group 2	0.47 ($p = 0.002$)	0.08 ($p = 0.6$)	0.03 ($p = 0.9$)	0.12 ($p = 0.5$)
A_{body}				
Group 1	0.32 ($p = 0.04$)	0.14 ($p = 0.4$)	0.10 ($p = 0.5$)	0.18 ($p = 0.3$)
Group 2	0.49 ($p = 0.001$)	0.08 ($p = 0.6$)	0.03 ($p = 0.8$)	0.13 ($p = 0.4$)
D_{body}				
Group 1	0.25 ($p = 0.1$)	0.12 ($p = 0.5$)	0.10 ($p = 0.5$)	0.19 ($p = 0.2$)
Group 2	0.19 ($p = 0.2$)	0.02 ($p = 0.9$)	0.01 ($p = 0.9$)	0.11 ($p = 0.5$)
AP				
Group 1	0.39 ($p = 0.01$)	0.07 ($p = 0.7$)	0.02 ($p = 0.9$)	0.17 ($p = 0.3$)
Group 2	0.45 ($p = 0.003$)	0.12 ($p = 0.5$)	0.07 ($p = 0.7$)	0.09 ($p = 0.6$)
D_{eff}				
Group 1	0.36 ($p = 0.02$)	0.10 ($p = 0.6$)	0.05 ($p = 0.7$)	0.20 ($p = 0.2$)
Group 2	0.41 ($p = 0.007$)	0.17 ($p = 0.3$)	0.12 ($p = 0.5$)	0.11 ($p = 0.5$)
LAT				
Group 1	0.21 ($p = 0.2$)	0.10 ($p = 0.5$)	0.09 ($p = 0.6$)	0.17 ($p = 0.3$)
Group 2	0.31 ($p = 0.049$)	0.17 ($p = 0.3$)	0.14 ($p = 0.4$)	0.22 ($p = 0.2$)
Age				
Group 1	0.34 ($p = 0.03$)	0.01 ($p = 1.0$)	0.05 ($p = 0.8$)	0.17 ($p = 0.3$)
Group 2	0.44 ($p = 0.004$)	0.05 ($p = 0.7$)	0.11 ($p = 0.5$)	0.08 ($p = 0.6$)

Table 5. Pearson Correlation Coefficients (*R*) between Radiation Dose Parameters and Image Quality Parameters

	Slice Thickness-Normalized Image Noise	SNR	CNR	Subjective Image Quality Grade
$CTDI_{vol}$ before CT scan				
Group 1	0.52 ($p = 0.0004$)	0.22 ($p = 0.2$)	0.17 ($p = 0.3$)	0.32 ($p = 0.04$)
Group 2	0.37 ($p = 0.02$)	0.01 ($p = 0.9$)	0.06 ($p = 0.7$)	0.19 ($p = 0.2$)
$CTDI_{vol}$ after CT scan				
Group 1	0.49 ($p = 0.001$)	0.21 ($p = 0.2$)	0.16 ($p = 0.3$)	0.30 ($p = 0.051$)
Group 2	0.20 ($p = 0.2$)	0.22 ($p = 0.2$)	0.26 ($p = 0.1$)	0.06 ($p = 0.7$)
Effective mAs				
Group 1	0.49 ($p < 0.0001$)	0.21 ($p = 0.2$)	0.16 ($p = 0.3$)	0.30 ($p = 0.054$)
Group 2	0.20 ($p = 0.2$)	0.23 ($p = 0.2$)	0.26 ($p = 0.1$)	0.06 ($p = 0.7$)
Quality reference mAs				
Group 1	0.04 ($p = 0.8$)	0.04 ($p = 0.8$)	0.01 ($p = 0.9$)	0.09 ($p = 0.6$)
Group 2	0.05 ($p = 0.8$)	0.24 ($p = 0.1$)	0.23 ($p = 0.1$)	0.24 ($p = 0.1$)

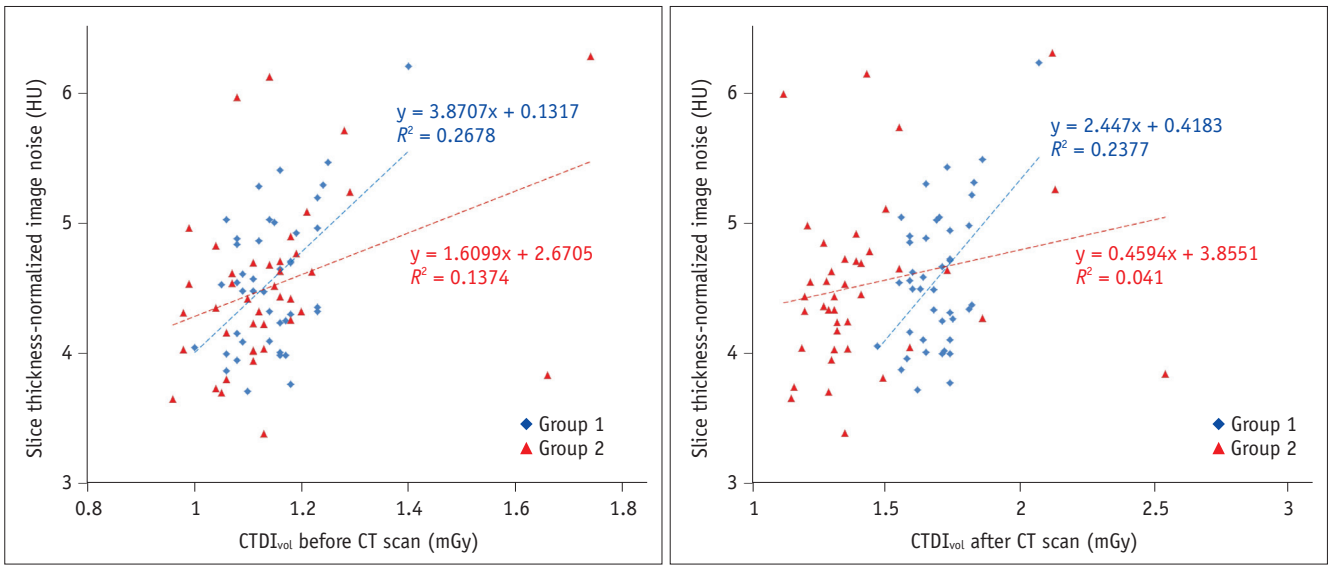

Fig. 5. Scatter plots demonstrating correlations between radiation dose and image noise of cardiothoracic CT.
A. In scatter plot, group 1 illustrates higher correlation (r = 0.52; p = 0.0004) between $CTDI_{vol}$ before CT scan and slice thickness-normalized image noise than that (r = 0.37; p = 0.02) in group 2. **B.** In scatter plot, group 1 illustrates modest correlation (r = 0.49; p = 0.001) between $CTDI_{vol}$ after CT scan and slice thickness-normalized image noise. In contrast, group 2 shows no significant correlation (r = 0.20; p = 0.2) between them that may be attributed to reduction of $CTDI_{vol}$ after CT scan, graphically recognized as leftward shift of red triangular points of group 2 in X-axis, compared with blue rhomboid points of group 1.

Table 6. Effect of Arm Position on Slice Thickness-Normalized Image Noise and Subjective Image Quality

	Arm Position					
	Both Up	Others	*P*	Both Horizontal	Others	*P*
Slice thickness-normalized image noise (HU)						
Group 1	4.5 ± 0.5 (n = 28)	4.7 ± 0.6 (n = 14)	0.1	4.7 ± 0.4 (n = 7)	4.5 ± 0.6 (n = 35)	0.6
Group 2	4.4 ± 0.6 (n = 25)	4.6 ± 0.7 (n = 16)	0.3	4.6 ± 0.7 (n = 9)	4.5 ± 0.6 (n = 32)	0.6
Subjective image quality grade						
Group 1	1.3 ± 0.4 (n = 28)	1.9 ± 0.7 (n = 14)	0.001	2.3 ± 0.5 (n = 7)	1.3 ± 0.5 (n = 35)	< 0.0001
Group 2	1.1 ± 0.3 (n = 25)	2.0 ± 0.5 (n = 16)	< 0.0001	2.2 ± 0.4 (n = 9)	1.3 ± 0.4 (n = 32)	< 0.0001

normalized image noise and subjective image quality grade (Table 5). All radiation dose parameters showed no significant correlations (p > 0.05) with SNR and CNR in both groups (Table 5). $CTDI_{vol}$ values before and after the CT scan and effective mAs demonstrated marginally significant correlations with subjective image quality grade in group 1, but no significant correlations (p > 0.05) were found between them in group 2 (Table 5).

Effect of Arm Position on Slice Thickness-Normalized Image Noise and Subjective Image Quality Grade

Arm position did not have a significant effect (p > 0.05) on slice thickness-normalized image noise (Table 6). In contrast, arm position had a significant effect (p ≤ 0.001) on subjective image quality grade: significantly higher image quality with both arms up compared with other arm positions and significantly lower image quality with horizontal position in both arms when compared with others (Table 6).

DISCUSSION

This study demonstrated that an additional reduction of radiation dose with comparable image noise could be achieved simply by changing the input steps of a user-determined radiation dose level in pediatric cardiothoracic CT with tube current modulation. This improved CT radiation dose optimization is attributable to a better adaptation of radiation dose to individual patient size and body habitus by using tube current modulation function more effectively in the new method (group 2). In the previous method (group 1), the $CTDI_{vol}$ determined by a single axial CT image was

Korean Journal of Radiology
KJR

used for the full scan range of cardiothoracic CT, which may be suboptimal in the optimization point of view and result in a CT radiation dose slightly higher than necessary for the user-determined image quality level. In contrast, the $CTDI_{vol}$ was initially entered for the minimal scan range at the same position as the axial CT image where the $CTDI_{vol}$ was calculated and the minimal range then was longitudinally extended to the full scan range of cardiothoracic CT in the new method (group 2). Although CT scanning is commonly performed with tube current modulation (4-8), such details of the input steps of radiation dose have not been evaluated or described. In this respect, the aforementioned result of this study is obviously a small step forward in CT radiation dose optimization that can be easily and widely used in our clinical practice. A lower or insignificant correlation between radiation dose and image noise in the group 2 than in the group 1 (Fig. 5) also would suggest a better CT radiation dose adaptation to patient size and habitus in group 2.

Among body size indices evaluated in this study, A_w showed the highest (r = 0.86–0.94) correlations with $CTDI_{vol}$ values before and after the CT scan as well as effective mAs in both groups, particularly between A_w and $CTDI_{vol}$ before the CT scan in the group 2 (r = 0.94). In this regard, the single best variable (A_w), instead of using a combination of two variables (A_{body} and mean D_{body}) as previously reported (14), can be used to develop a new best fit equation using this high linear relationship between the two for estimating a better body size-adapted CT radiation dose prior to CT scanning. Compared with A_w in this study, A_{body} showed a lower correlation (r = 0.73; p < 0.001) in the group using 80 kVp in the previous study (14). On the contrary, D_{body} showed no significant correlation in this study and the previous study (14). Recent studies also have shown that an attenuation-based method, such as A_w or water equivalent diameter, is superior to geometric parameters. This is especially true in the thoracic region demonstrating a greater difference in CT numbers than other regions due to the inclusion of the lung, for estimating patient size that can be used to determine optimal CT radiation dose (12, 13, 17-20).

The attenuation-based patient size can be obtained from CT scout image or axial CT images. The method using CT scout image is limited by a complicated calibration process of pixel values using a series of water phantoms, a non-edge enhanced image filter that are not currently available from all manufacturers, and magnification errors caused by patient miscentering (13). On the other hand, the method using axial CT images can only be performed after the CT scan is finished and, therefore, cannot be used to determine a user-defined image quality level prior to the CT scan (13). Moreover, frequent image truncation on clinical CT images leads to incomplete extraction of the whole patient cross section (20). The CT image-based method requires a threshold-based segmentation to extract A_{body} and D_{body} necessary for calculating A_w as in this study. When manual drawing of a region of interest was performed to include the whole patient cross section for the axial CT image, care was taken to exclude the patient table and other attenuating materials in this study. In the previous study (13), inclusion of the patient table led to overestimation of an attenuation-based patient size measure, particularly for pediatric patients due to their relatively small size, up to 45.7%. On the contrary, the patient table was not included in the patient cross section in this study by using a careful manual drawing of a region of interest. As a result, potential overestimation of A_w could be completely avoided. It is noteworthy that the manual drawing of a region of interest necessary for excluding the patient table, however, makes automated calculations of an attenuation-based patient size difficult.

In this study, subjective image quality in the shoulder regions was frequently degraded by a horizontal arm position. Arm position on a CT scout image is important to avoid an unexpectedly high radiation dose from a CT scan with tube current modulation. In this regard, the position with both arms up is recommended for this reason (6, 7, 21). Nonetheless, both arms could not be raised up in all the patients in this study due to a risk of patient movement and awakening when both arms were raised up in some patients (34% in the group 1 and 39% in the group 2). Increased radiation dose, caused by arm position on CT scout image, could not be evaluated because patients with different arm positions had different patient sizes and body densities in this study. The degraded image quality caused by a horizontal arm position and localized in the shoulder regions in this study was thought to result from tube current saturation in those regions. Tube current saturation occurred in thick body regions, e.g., the shoulder, also diminishes the dose saving effect of tube current modulation especially at low kVp or fast scan speed (5, 22, 23). No significant effect of arm position on image noise in this study seemed to be misleading because image noise was not measured in the shoulder regions showing

the degraded image quality.

A recent multi-center, multi-vendor study on radiation dose of pediatric cardiac CT (24) clearly demonstrates a further demand for CT radiation dose optimization. In this regard, the results of this study would be beneficial in the optimization process. The previous study using the same best fit equation (14) showed considerably higher image noise (approximately 13.7 HU) than this study (approximately 4.6 HU). The lower image noise in this study might be mainly due to the use of iterative reconstruction algorithm instead of conventional filtered back projection. Based on the results of this study, radiation dose of pediatric cardiothoracic CT in our institution was reduced by 15%. In addition, it is planned to use the $CTDI_{vol}$ value individually determined prior to CT scan by using the A_w only rather than a combination of A_{body} and mean D_{body} for further CT radiation dose optimization because the former showed the highest correlation with X-ray outputs of CT scans in this study.

This study has several limitations. First, the unpaired comparison between the two groups in this retrospective study might introduce an imperfect statistical comparison, compared with paired comparison. However, paired comparison between the two methods in the same patient may be regarded unethical in young children because two CT exams in the same patient inevitably double radiation risks. As an alternative, the paired comparison can be tested by using an anthropomorphic phantom in a future study. Nevertheless, the unpaired comparison in this study might not cause a substantial statistical error because the independent variables including patient age, body parameters, and arm position on a CT scout image were comparable between the two groups. Second, to ensure patient centering in vertical direction, a lateral scout image is very useful (6, 16, 19). Because only anterolateral scout image was used in this study, a potential error in patient centering might affect the CT X-ray outputs and radiation exposure to patient in this study using tube current modulation and a bowtie filter (16, 25). However, technologists used the same protocol for positioning patients in the isocenter in the two groups in this study. A radiolucent pad was additionally placed on the CT table to compensate for a low vertical position of a smaller patient in this study because the low position was reported to be particularly pronounced in smaller children (16). Furthermore, the center of body actually depends on the z-location and therefore cannot be at the same isocenter for the entire longitudinal scan range (16). Third, the results of this study were obtained in a single CT manufacturer. Therefore, different results may be obtained in others. Last, size-specific dose estimate or effective dose of pediatric cardiothoracic CT was not calculated because this study was not aimed to estimate CT radiation dose but to compare the two different methods in CT radiation dose optimization.

In conclusion, the $CTDI_{vol}$ entered before scan range adjustment provides a significant radiation dose reduction (18%) with comparable image noise in pediatric cardiothoracic CT with tube current modulation, compared with that entered after scan range adjustment.

REFERENCES

1. Greenwood TJ, Lopez-Costa RI, Rhoades PD, Ramírez-Giraldo JC, Starr M, Street M, et al. CT dose optimization in pediatric radiology: a multiyear effort to preserve the benefits of imaging while reducing the risks. *Radiographics* 2015;35:1539-1554
2. Goo HW. CT radiation dose optimization and estimation: an update for radiologists. *Korean J Radiol* 2012;13:1-11
3. Goo HW. State-of-the-art CT imaging techniques for congenital heart disease. *Korean J Radiol* 2010;11:4-18
4. Greess H, Lutze J, Nömayr A, Wolf H, Hothorn T, Kalender WA, et al. Dose reduction in subsecond multislice spiral CT examination of children by online tube current modulation. *Eur Radiol* 2004;14:995-999
5. Goo HW, Suh DS. Tube current reduction in pediatric non-ECG-gated heart CT by combined tube current modulation. *Pediatr Radiol* 2006;36:344-351
6. Cody DD. Management of auto exposure control during pediatric computed tomography. *Pediatr Radiol* 2014;44 Suppl 3:427-430
7. Söderberg M. Overview, practical tips and potential pitfalls of using automatic exposure control in CT: Siemens CARE Dose 4D. *Radiat Prot Dosimetry* 2016;169:84-91
8. Solomon JB, Li X, Samei E. Relating noise to image quality indicators in CT examinations with tube current modulation. *AJR Am J Roentgenol* 2013;200:592-600
9. Jung YY, Goo HW. The optimal parameter for radiation dose in pediatric low dose abdominal CT: cross-sectional dimensions versus body weight. *J Korean Radiol Soc* 2008;58:169-175
10. Dong F, Davros W, Pozzuto J, Reid J. Optimization of kilovoltage and tube current-exposure time product based on abdominal circumference: an oval phantom study for pediatric abdominal CT. *AJR Am J Roentgenol* 2012;199:670-676
11. Menke J. Comparison of different body size parameters for individual dose adaptation in body CT of adults. *Radiology* 2005;236:565-571
12. Wang J, Duan X, Christner JA, Leng S, Yu L, McCollough CH. Attenuation-based estimation of patient size for the purpose

of size specific dose estimation in CT. Part I. Development and validation of methods using the CT image. *Med Phys* 2012;39:6764-6771
13. Wang J, Christner JA, Duan X, Leng S, Yu L, McCollough CH. Attenuation-based estimation of patient size for the purpose of size specific dose estimation in CT. Part II. Implementation on abdomen and thorax phantoms using cross sectional CT images and scanned projection radiograph images. *Med Phys* 2012;39:6772-6778
14. Goo HW. Individualized volume CT dose index determined by cross-sectional area and mean density of the body to achieve uniform image noise of contrast-enhanced pediatric chest CT obtained at variable kV levels and with combined tube current modulation. *Pediatr Radiol* 2011;41:839-847
15. Goo HW, Allmendinger T. Combined electrocardiography- and respiratory-triggered CT of the lung to reduce respiratory misregistration artifacts between imaging slabs in free-breathing children: initial experience. *Korean J Radiol* 2017;18:860-866
16. Kaasalainen T, Palmu K, Reijonen V, Kortesniemi M. Effect of patient centering on patient dose and image noise in chest CT. *AJR Am J Roentgenol* 2014;203:123-130
17. Larson DB, Wang LL, Podberesky DJ, Goske MJ. System for verifiable CT radiation dose optimization based on image quality. part I. Optimization model. *Radiology* 2013;269:167-176
18. Larson DB, Malarik RJ, Hall SM, Podberesky DJ. System for verifiable CT radiation dose optimization based on image quality. part II. Process control system. *Radiology* 2013;269:177-185
19. Li B, Behrman RH, Norbash AM. Comparison of topogram-based body size indices for CT dose consideration and scan protocol optimization. *Med Phys* 2012;39:3456-3465
20. Ikuta I, Warden GI, Andriole KP, Khorasani R, Sodickson A. Estimating patient dose from x-ray tube output metrics: automated measurement of patient size from CT images enables large-scale size-specific dose estimates. *Radiology* 2014;270:472-480
21. Kuo F, Plaza M, Saigal G. Inappropriate arm positioning during scout image acquisition resulting in increased radiation dose while performing a chest CT. *Pediatr Radiol* 2012;42:508-509
22. Goo HW, Suh DS. The influences of tube voltage and scan direction on combined tube current modulation: a phantom study. *Pediatr Radiol* 2006;36:833-840
23. Israel GM, Herlihy S, Rubinowitz AN, Cornfeld D, Brink J. Does a combination of dose modulation with fast gantry rotation time limit CT image quality? *AJR Am J Roentgenol* 2008;191:140-144
24. Hui PKT, Goo HW, Du J, Ip JJK, Kanzaki S, Kim YJ, et al. Asian consortium on radiation dose of pediatric cardiac CT (ASCI-REDCARD). *Pediatr Radiol* 2017;47:899-910
25. Toth T, Ge Z, Daly MP. The influence of patient centering on CT dose and image noise. *Med Phys* 2007;34:3093-3101